# A Mixed Logical Dynamics Actuator Model for Optimal Control with Position and Rate Limits * **

Rubens J. M. Afonso[1,2][0000−0001−9209−2253],
Johannes Diepolder[1][0000−0002−5962−6126], and
Florian Holzapfel[1][0000−0003−4733−9186]

[1] Institute of Flight System Dynamics, Technische Universität München, Garching bei München, Germany
{rubens.afonso,johannes.diepolder,florian.holzapfel}@tum.de

[2] Electronic Engineering Division, Instituto Tecnológico de Aeronáutica, São José dos Campos, Brazil rubensjm@ita.br



**Abstract.** In this paper the solution of optimal control problems under actuator excursion and rate limits is considered. One way of addressing internal limits of a servomechanism in optimal control problems is through the introduction of input and state constraints. However, this modeling approach may introduce unnecessary conservatism in the optimal solution of the control problem. In the present work an actuator formulation based on Mixed Logical Dynamics (MLD) is developed to address this issue, eliminating the conservatism. These conditions are implemented through a Mixed-Integer Linear Programming (MILP) formulation with binary variables. The application of the formulation is illustrated using a model of a general transport aircraft. In this scenario both the standard optimal control formulation with state constraints and the novel MILP formulation proposed in this paper are used to maximize a heading change of the aircraft at a fixed terminal time. It is shown that the MILP encoding yields a lower cost function value compared to the standard optimal control formulation at the expense of greater computational resources.

**Keywords:** Mixed logical dynamics · Mixed integer linear programming · Actuator limits · Aircraft control

* Rubens Afonso acknowledges the support of CAPES (fellowship proc. #88881.145490/2017-01) and the Federal Ministry for Education and Research of Germany through the Alexander von Humboldt Foundation. Johannes Diepolder acknowledges the support by the DFG grant HO4190/8-2.

# 1 Introduction

Actuator saturations are ubiquitously present in control systems and limit the capacity of steering the plant. Such saturations usually originate from the physics of the operation of the actuators, e.g. the aperture of a valve, which cannot lie outside the interval between 0 and 100%. Hence, even if the controller commands an aperture of 110%, this is not physically achievable. If left unaddressed by the controller, such limitations may compromise the performance or even the stability of the closed-loop system (see e.g. [10]). Therefore, it is important to consider these limitations within the design of control laws.

In the optimal control framework, actuator rate or excursion saturations are usually modeled via reformulation of such limitations as constraints within the optimization problem, as in [6]. Therefore, the optimal control is determined so that these constraints are not violated. On the other hand, the saturations are enforced by the actuators themselves in practice, even if the controls are not determined to respect them. This effectively limits the set of candidate solutions to the optimization problem to those that do not violate the constraints *a priori*, whereas in reality no solution would violate these constraints by their very nature. This simplified modeling approach does not come without cost, as the limitation *a priori* may entail suboptimal solutions [4].

For example, consider a valve: even if the control entails an aperture of more than 100% of its capacity, such an aperture cannot be physically achieved. Furthermore, suppose that the same control command is sent to other elements in the control loop. One can hypothesize that the same command is used to drive a heater whose limits are not reached by the same command value that would entail an aperture of 110% of the valve. Therefore, by using a command that is smaller in magnitude so that the valve is not steered to open more than 100% *a priori*, one is also limiting the output of the heater, yielding a possibly suboptimal solution. In contrast, the saturation of the valve can be considered in a hybrid model, in which it behaves linearly between 0% and 100%, but does not leave this interval in spite of commands in that sense. Then, the command could exceed the corresponding value and the heater might be driven to its optimal state, thus enabling an optimal solution to the real control problem. In other words, if the control could be chosen freely on such constrained arcs of the more limited actuator, then it could optimally command the remaining one.

In the present paper, the optimal control problem involves deciding commands that drive actuators in closed-loop. An aircraft model is used and focus is given in the lateral motion, with the actuators being the left and right ailerons, the rudder, as well as the elevator. Each of these control surfaces is modeled as a second-order system, driven by the references of the heading as well as the normal and lateral load factors. The lateral acceleration is regulated to zero throughout the maneuver and the aim is to optimize the heading command to achieve the maximum heading change within a given fixed time interval. The excursion of the control surface actuators and their rates of change are limited. Moreover, a fault is assumed to take place in the left aileron, whereas the right one as well as the rudder and elevator operate normally. This fault results in a severely reduced excursion for the affected surface. This gives rise to the kind of problem discussed above, as the saturation is usually modeled by state constraints in the optimal control problem, leading to unnecessary conservatism. An early example of such modeling in the context of aircraft control using Linear Programming can be found in [8]. Another example can be found in [2], where the fault is a jamming of one surface, which leads to a necessity of performing a different control allocation to the remaining actuators.

In this work, the actuator saturations are modeled as physical limits that are imposed *a posteriori*, i.e., the excursion is saturated if the command would lead to a violation. The proposed optimization problem considers the saturation, but does not regard it as an state constraint, rather treats it using logic: whenever the limit is to be exceeded, it is saturated and the derivative is set to zero. Thus, the proposed approach is not as conservative as the usual modeling using state constraints, but yields an optimization problem that takes the saturation into account.

The presence of logical clauses in the optimization problem leads to a Mixed Logical Dynamics (MLD) model, as the control and state variables are subject to the continuous-time dynamics of the aircraft and servomechanisms, whereas the saturations introduce logical switching between linear models for the actuators. For implementing the logic, binary optimization variables are used in conjunction with the real-valued variables representing the controls and states. The presence of these binary variables entails a Mixed-Integer Linear Programming (MILP) problem, a class known to be NP-Complete [5]. Consequently, it is expected that the computational cost is increased as compared to the usual optimal control formulation. Therefore, in the proposal the number of binary variables is reduced by blocking them for a number of successive time steps, which than introduces a compromise between optimality and computational burden.

The remainder of the present paper is divided as follows. The usual formulation as an Optimal Control Problem (OCP) and the proposed MLD reformulation are presented in Section 2. The aircraft model for the illustrative example considered in this work is outlined in Section 3. Simulation results comparing the proposal and the usual OCP are shown and discussed in Section 4. Finally, concluding remarks and suggestion for future work are given in Section 5.

# 2 Optimal Control Problem Formulations

## 2.1 Optimal Control Formulation with Bounded Actuator States

Let us first introduce an optimal control problem formulation which considers actuator limits using purely state dependent constraints. The discrete Linear-Time-Invariant (LTI) model is defined as

$$\mathbf{x}_{k+1} = \mathbf{A}_d \mathbf{x}_k + \mathbf{B}_d \mathbf{u}_k,\ \ k = 0, \ldots, N-1, \tag{1}$$

with the state vectors $\mathbf{x}_k \in \mathbb{R}^m$ and $\mathbf{x}_{k+1} \in \mathbb{R}^m$ corresponding to the instants $t_k$ and $t_{k+1}$, the control vector $\mathbf{u}_k \in \mathbb{R}^n$ at instant $t_k$ as well as the discrete system matrix $\mathbf{A}_d \in \mathbb{R}^{m\times m}$ and the discrete input matrix $\mathbf{B}_d \in \mathbb{R}^{m\times n}$. The controls are assumed to be constrained by box bounds of the form:

$$\mathbf{u}_{lb} \leq \mathbf{u}_k \leq \mathbf{u}_{ub}. \tag{2}$$

If the actuator position and rate limits are introduced as purely state dependent constraints in the optimal control problem the state variables at time points $t_k,\ k = 1, \ldots, N$ are subject to general limits:

$$\mathbf{x}_{lb} \leq \mathbf{x}_k \leq \mathbf{x}_{ub}. \tag{3}$$

In order to simplify notation the components in the vector $\mathbf{x}_{lb}$ ($\mathbf{x}_{ub}$) are set to $-\infty$ ($+\infty$) for all unbounded states. The initial state $\mathbf{x}_0$ is fixed to the initial condition

$$\mathbf{x}_0 = \mathbf{x}(t_0) \tag{4}$$

and the Mayer type cost function is modeled using a linear combination $\mathbf{c}^T\mathbf{x}_N, \mathbf{c} \in \mathbb{R}^m$ of the state vector components at the final state $\mathbf{x}_N$. Moreover, final boundary conditions may be imposed on the state at the terminal time point $t_N$:

$$\mathbf{x}_{f,lb} \leq \mathbf{x}_N \leq \mathbf{x}_{f,ub}. \tag{5}$$

Similarly to the state constraints, the limits of all unbounded states $\mathbf{x}_{f,lb}$ ($\mathbf{x}_{f,ub}$) are set to $-\infty$ ($+\infty$).

Considering the optimal control problem on a horizon of $N$ time-steps the linear problem formulation is:

$$\begin{aligned} \underset{\mathbf{x}_N, \mathbf{x}_k, \mathbf{u}_k, k=0,\ldots,N-1}{\text{minimize}} \quad & \mathbf{c}^T\mathbf{x}_N \\ \text{subject to} \quad & \mathbf{A}_d\mathbf{x}_k + \mathbf{B}_d\mathbf{u}_k - \mathbf{x}_{k+1} = \mathbf{0},\ k = 0, \ldots, N-1, \\ & \mathbf{x}_0 = \mathbf{x}(t_0), \\ & \mathbf{x}_{f,lb} \leq \mathbf{x}_N \leq \mathbf{x}_{f,ub}, \\ & \mathbf{x}_{lb} \leq \mathbf{x}_k \leq \mathbf{x}_{ub},\ k = 1, \ldots, N, \\ & \mathbf{u}_{lb} \leq \mathbf{u}_k \leq \mathbf{u}_{ub},\ k = 0, \ldots, N-1. \end{aligned} \tag{6}$$

## 2.2 Mixed Logical Dynamics Actuator Model

Next, an actuator model based on a MLD formulation for a linear system

$$x_{v,k+1} = \mathbf{a}_v^T\mathbf{x}_k + \mathbf{b}_v^T\mathbf{u}_k \tag{7}$$

$$x_{p,k+1} = \mathbf{a}_p^T\mathbf{x}_k + \mathbf{b}_p^T\mathbf{u}_k \tag{8}$$

with the system vectors $\mathbf{a}_v \in \mathbb{R}^m$ and $\mathbf{a}_p \in \mathbb{R}^m$ as well as the input vectors $\mathbf{b}_v \in \mathbb{R}^n$ as well as $\mathbf{b}_p \in \mathbb{R}^n$ is introduced. Moreover, the states $x_v$ and $x_p$ are components of the state vector $\mathbf{x}$. Five different cases are distinguished regarding the actuator limits using four binary decision variables $d_{i,k} \in \{0,1\}, i \in \{1,2,3,4\}$ for each of the instants $t_k,\ k = 1,\ldots,N$. At each time-step $t_k$ only one of the decision variables $d_{1,k}$, $d_{2,k}$, $d_{3,k}$, or $d_{4,k}$ is allowed to be one, i.e. either one of the decision variables is one and the others are all zero or all decision variables are zero. In the following, the first binary variable $d_{1,k}$ corresponds to the lower rate limit and the second variable $d_{2,k}$ corresponds to the upper rate limit. Similarly, the third variable $d_{3,k}$ corresponds to the lower position limit and the fourth variable $d_{4,k}$ corresponds to the upper position limit. If any of these variables is chosen as one the corresponding rate or position limit is regarded as active. If all variables are zero the actuator is unbounded and evolves according to the linear model defined in Eqs. (7) and (8). It is important to emphasize that the binary variables cannot be treated as free variables in view of the coupling with the states by the implications introduced in Alg. 1. For example, if $d_{1,k} = 1$ at some time instant $t_k$, then the corresponding constraints in lines 5–7 would have to be satisfied, which may not be feasible due to the current state of the system.

In the following, the equality and inequality constraints which need to be introduced for the actuator model depending on the values of the decision variables at each discrete time point are described. Let $\mathcal{C}_{eq}$ denote a set of functions which collects all equality constraints related to the actuator model. Similarly, let $\mathcal{C}_{iq}$ denote a set of functions for all inequality constraints.

Depending on the choice of the binary variables $d_{i,k}, i = 1,2,3,4$ for each time-step $t_k \to t_{k+1}$ the constraints which need to be added to these sets are described in Alg. 1. This procedure is called for all $k \in \{0,\ldots,N-1\}$ in a loop and updates the equality and inequality constraints in the sets $\mathcal{C}_{eq}$ and $\mathcal{C}_{iq}$ (both initialized as empty sets before the first iteration of the loop). Note that the anticipated rate and position states $\tilde{x}_p$ and $\tilde{x}_v$ (cf. lines 2 and 3 in Alg. 1) are not components of the state vector. They are rather predictions without considering the effect of the saturations. Observe that the last constraint which is added to the set $\mathcal{C}_{iq}$ of inequality constraints

$$d_{1,k} + d_{2,k} + d_{3,k} + d_{4,k} - 1 \leq 0 \tag{9}$$

ensures together with $d_{i,k} \in \{0,1\}, i = 1,2,3,4$ that either all decision variables are zero or at most a single variable is one. To model the logical conditions from Alg. 1 in a Linear Program the big-M formulation is employed [1, 3].

Note that all constraint functions $c : \mathbb{R}^p \to \mathbb{R}$ are of the general form

$$c(\mathbf{z}_c) = \mathbf{a}_c^T \mathbf{z}_c - b_c,$$

with a parameter vector $\mathbf{z}_c \in \mathbb{R}^p$, a constraint vector $\mathbf{a}_c \in \mathbb{R}^p$ as well as the scalar right-hand-side $b_c \in \mathbb{R}$. For an inequality constraint function $c(\mathbf{z}_c) \leq 0$ the big-M formulation can be written as

$$c(\mathbf{z}_c) \leq \mathcal{C}(\mathbf{d})\mathcal{M}(c(\mathbf{z}_c)),$$

where $\mathcal{C}(\mathbf{d})$ is a condition depending on a vector of binary variables $\mathbf{d}$ which takes either the value true or false (respectively zero or one) and $\mathcal{M}(c(\mathbf{z}_c))$ returns a

**Algorithm 1** Actuator model constraints

**procedure** C($\mathcal{C}_{eq}, \mathcal{C}_{iq}, d_{1\ldots4,k}, \mathbf{x}_k, \mathbf{x}_{k+1}, \mathbf{u}_k, \mathbf{a}_v, \mathbf{a}_p, \mathbf{b}_v, \mathbf{b}_p, x_{v,lb}, x_{v,ub}, x_{p,lb}, x_{p,ub}$)
▷ Add actuator constraints for a time-step $t_k \rightarrow t_{k+1}$
  $\tilde{x}_v \leftarrow \mathbf{a}_v^T \mathbf{x}_k + \mathbf{b}_v^T \mathbf{u}_k$ ▷ Predicted rate state
  $\tilde{x}_p \leftarrow \mathbf{a}_p^T \mathbf{x}_k + \mathbf{b}_p^T \mathbf{u}_k$ ▷ Predicted position state
  **if** $d_{1,k}$ **then**
    $\mathcal{C}_{iq} \leftarrow \mathcal{C}_{iq} \cup \{\tilde{x}_v - x_{v,lb} \leq 0\}$
    $\mathcal{C}_{eq} \leftarrow \mathcal{C}_{eq} \cup \{x_{v,k+1} - x_{v,lb} = 0\}$
    $\mathcal{C}_{eq} \leftarrow \mathcal{C}_{eq} \cup \{x_{p,k+1} - \mathbf{a}_p^T \mathbf{x}_k - \mathbf{b}_p^T \mathbf{u}_k = 0\}$
  **else if** $d_{2,k}$ **then**
    $\mathcal{C}_{iq} \leftarrow \mathcal{C}_{iq} \cup \{-\tilde{x}_v + x_{v,ub} \leq 0\}$
    $\mathcal{C}_{eq} \leftarrow \mathcal{C}_{eq} \cup \{-x_{v,k+1} + x_{v,ub} = 0\}$
    $\mathcal{C}_{eq} \leftarrow \mathcal{C}_{eq} \cup \{x_{p,k+1} - \mathbf{a}_p^T \mathbf{x}_k - \mathbf{b}_p^T \mathbf{u}_k = 0\}$
  **else if** $d_{3,k}$ **then**
    $\mathcal{C}_{iq} \leftarrow \mathcal{C}_{iq} \cup \{\tilde{x}_p - x_{p,lb} \leq 0\}$
    $\mathcal{C}_{iq} \leftarrow \mathcal{C}_{iq} \cup \{\tilde{x}_v \leq 0\}$
    $\mathcal{C}_{eq} \leftarrow \mathcal{C}_{eq} \cup \{x_{p,k+1} - x_{p,lb} = 0\}$
    $\mathcal{C}_{eq} \leftarrow \mathcal{C}_{eq} \cup \{x_{v,k+1} = 0\}$
  **else if** $d_{4,k}$ **then**
    $\mathcal{C}_{iq} \leftarrow \mathcal{C}_{iq} \cup \{-\tilde{x}_p + x_{p,ub} \leq 0\}$
    $\mathcal{C}_{iq} \leftarrow \mathcal{C}_{iq} \cup \{-\tilde{x}_v \leq 0\}$
    $\mathcal{C}_{eq} \leftarrow \mathcal{C}_{eq} \cup \{-x_{p,k+1} + x_{p,ub} = 0\}$
    $\mathcal{C}_{eq} \leftarrow \mathcal{C}_{eq} \cup \{x_{v,k+1} = 0\}$
  **else**
    $\mathcal{C}_{eq} \leftarrow \mathcal{C}_{eq} \cup \{x_{p,k+1} - \mathbf{a}_p^T \mathbf{x}_k - \mathbf{b}_p^T \mathbf{u}_k = 0\}$
    $\mathcal{C}_{eq} \leftarrow \mathcal{C}_{eq} \cup \{x_{v,k+1} - \mathbf{a}_v^T \mathbf{x}_k - \mathbf{b}_v^T \mathbf{u}_k = 0\}$
  **end if**
  $\mathcal{C}_{iq} \leftarrow \mathcal{C}_{iq} \cup \{d_{1,k} + d_{2,k} + d_{3,k} + d_{4,k} - 1 \leq 0\}$
**return** $\mathcal{C}_{eq}, \mathcal{C}_{iq}$
**end procedure**

conservative big-M constant for relaxing the constraint. For this big-M constant it needs to be ensured that given an admissible region $\mathcal{Z}_c$ for the parameters $\mathbf{z}_c$ the value of the constraint function is always lower than this constant. The minimum cost function value of the following Linear Program $\mathcal{M}(c(\mathbf{z}_c))$

$$\underset{\mathbf{z}_c \in \mathcal{Z}_c}{\text{minimize}} \quad -c(\mathbf{z}_c)$$

yields the maximum value of the constraint function. However, it remains to determine the admissible set $\mathcal{Z}_c$ for the parameters $\mathbf{z}_c$. Observe that for all constraints the vector $\mathbf{z}_c$ merely contains the discretized control and state variables. As such, the admissible set is defined by the limits of these variables. For the controls these limits are readily available as all inputs to the system are assumed bounded (cf. Eq. (2)). The same holds for the bounded state variables (cf. Eq. (3)). For the unbounded state variables $x_i, i \in \mathcal{I} := \{i : x_{lb,i} = -\infty \text{ or } x_{ub,i} = +\infty\}$ conservative limits can be determined from the following Linear Program $\mathcal{B}(m, i)$

$$\begin{aligned}
\underset{\mathbf{x}_N, \mathbf{x}_k, \mathbf{u}_k, k=0,\ldots,N-1}{\text{minimize}} \quad & m\mathbf{e}_i^T \mathbf{x}_N \\
\text{subject to} \quad & \mathbf{A}_d \mathbf{x}_k + \mathbf{B}_d \mathbf{u}_k - \mathbf{x}_{k+1} = \mathbf{0},\ k = 0, \ldots, N-1, \\
& \mathbf{x}_0 = \mathbf{x}(t_0), \\
& \mathbf{u}_{lb} \leq \mathbf{u}_k \leq \mathbf{u}_{ub},\ k = 0, \ldots, N-1,
\end{aligned}$$

where $m = 1$ for a minimization, i.e. a determination of the lower limit, and $m = -1$ for a maximization, i.e. a determination of the upper limit. Moreover, $\mathbf{e}_i$ denotes a vector which only has a unit entry at the $i$-th component and zero at the remaining components. Here, we require $\mathbf{x}(t_0)$ to be an equilibrium point of the system.

The extension to equality constraints is straight-forward due to the fact that an equality constraint may be expressed using two inequality constraints

$$\begin{aligned}
c(\mathbf{z}_c) &\leq \mathcal{C}(\mathbf{d})\mathcal{M}(c(\mathbf{z}_c)), \\
-c(\mathbf{z}_c) &\leq \mathcal{C}(\mathbf{d})\mathcal{M}(-c(\mathbf{z}_c))
\end{aligned}$$

and the same procedure for the computation of the big-M constant can be employed for each of the inequality constraints. For completeness, the full list of constraints including the corresponding conditions which need to be introduced using the big-M notation is provided in Table 1.

**Table 1.** Constraints and conditions introduced for each time step $t_k \to t_{k+1}$ using the big-M notation. The conditions are true if the expressions return zero.

| Constraints $\mathbf{c}(\mathbf{z}_c)$ | Conditions $\mathcal{C}(\mathbf{d})$ |
|---|---|
| $\tilde{x}_v - x_{v,lb} \leq 0$ | $1 - d_{1,k}$ |
| $x_{v,k+1} - x_{v,lb} = 0$ | $1 - d_{1,k}$ |
| $-\tilde{x}_v + x_{v,ub} \leq 0$ | $1 - d_{2,k}$ |
| $-x_{v,k+1} + x_{v,ub} = 0$ | $1 - d_{2,k}$ |
| $x_{p,k+1} - \mathbf{a}_p^T \mathbf{x}_k - \mathbf{b}_p^T \mathbf{u}_k = 0$ | $1 - d_{1,k} - d_{2,k}$ |
| $\tilde{x}_p - x_{p,lb} \leq 0$ | $1 - d_{3,k}$ |
| $\tilde{x}_v \leq 0$ | $1 - d_{3,k}$ |
| $x_{p,k+1} - x_{p,lb} = 0$ | $1 - d_{3,k}$ |
| $-\tilde{x}_p + x_{p,ub} \leq 0$ | $1 - d_{4,k}$ |
| $-\tilde{x}_v \leq 0$ | $1 - d_{4,k}$ |
| $-x_{p,k+1} + x_{p,ub} = 0$ | $1 - d_{4,k}$ |
| $x_{v,k+1} = 0$ | $1 - d_{3,k} - d_{4,k}$ |
| $x_{p,k+1} - \mathbf{a}_p^T \mathbf{x}_k - \mathbf{b}_p^T \mathbf{u}_k = 0$ | $d_{1,k} + d_{2,k} + d_{3,k} + d_{4,k}$ |
| $x_{v,k+1} - \mathbf{a}_v^T \mathbf{x}_k - \mathbf{b}_v^T \mathbf{u}_k = 0$ | $d_{1,k} + d_{2,k} + d_{3,k} + d_{4,k}$ |

# 3 Aircraft Model

The dynamic model under consideration represents the closed-loop system of a generic twin-engine, fixed-wing aircraft. The plant, which is described as a rigid body, is controlled by the primary control surfaces, i.e. the left and right ailerons as well as the elevator and the rudder. The inner-loop controller for this aircraft features integral as well as proportional parts and translates a roll angle command $\Phi_c$, as well as normal and lateral load factor commands, $n_{z,c}$ and $n_{y,c}$, to desired control surface deflections. For each of the primary control surfaces (ailerons, elevator, and rudder) the dynamics are modeled by linear second-order models (natural frequency $\omega_n = 40\,\mathrm{rad/s}$, relative damping $\bar{\zeta} = 0.707$) of the form

$$\frac{d}{dt}\begin{bmatrix} x(t) \\ \dot{x}(t) \end{bmatrix} = \begin{bmatrix} 0 & 1 \\ -\omega_n^2 & -2\bar{\zeta}\omega_n \end{bmatrix} \begin{bmatrix} x(t) \\ \dot{x}(t) \end{bmatrix} + \begin{bmatrix} 0 \\ k_a \end{bmatrix} \delta(t), \tag{10}$$

with a commanded value $\delta(t)$ which is fed from the controller to the actuators with an input gain $k_a$. Note that this model is of the same form assumed in the MLD formulation upon discretization (cf. Eqs. (7) and (8)). In the present work, the dynamics are discretized using a forward Euler approximation [7]. The complete closed-loop aircraft model including the plant, actuator models, and the inner-loop controller can be described by a nonlinear state space model:

$$\dot{\mathbf{x}}(t) = \mathbf{f}\left(\mathbf{x}(t), \mathbf{u}(t)\right). \tag{11}$$

Tables 2 and 3 summarize the states and controls considered in this model respectively. The linear model considered for the optimization is obtained through a linearization of the nonlinear model (11) at a horizontal reference flight condition (reference height 2500 m, reference velocity 67 m/s). For our analysis, the thrust command is assumed to be held at the respective trim value at all times. Moreover, a decoupling between the longitudinal and lateral modes is assumed, so that the optimization considers only the lateral motion. Later, the generated inputs by the proposed approach in the present paper are fed to the complete nonlinear model for validation.

It is important to mention that this particular model assumes a single actuator for the ailerons, as one considers that symmetric commands are sent to the left and right ailerons. In the present work, the left aileron is assumed to be in a fault condition, which limits its excursion severely more than the nominal one, whereas the right aileron and the rudder operate under nominal conditions. Therefore, in order to separate both ailerons, left and right deflections $\xi_l$ and $\xi_r$, as well as rates $\dot{\xi}_l$ and $\dot{\xi}_r$, respectively, are considered instead of a single deflection $\xi$ and rate $\dot{\xi}$. Their effect is taken into account by hypothesizing that each of these deflections generate half of the moment that would be generated by an equivalent $\xi$. Therefore, their coefficient is half of the coefficient of $\xi$ and then their deflections are summed. Under nominal operation, i.e., when both ailerons are subject to the same limits, this should yield the same result as a single aileron symmetric deflection variable applied to them.

**Table 2.** States of the aircraft model.

| Model | State Name | Symbol |
|---|---|---|
| Longitudinal | Integral of the load factor error | $I_{n_z}$ |
| | Speed | $V$ |
| | Angle of attack | $\alpha$ |
| | Pitch rate | $\omega_y$ |
| | Pitch angle | $\theta$ |
| | Elevator rate | $\dot{\eta}$ |
| | Elevator deflection | $\eta$ |
| | Height | $h$ |
| Lateral | Sideslip angle | $\beta$ |
| | Roll rate | $\omega_x$ |
| | Yaw rate | $\omega_z$ |
| | Roll angle | $\Phi$ |
| | Yaw angle | $\Psi$ |
| | Aileron rate | $\dot{\xi}$ |
| | Aileron deflection | $\xi$ |
| | Rudder rate | $\dot{\zeta}$ |
| | Rudder deflection | $\zeta$ |
| | Integral of the roll angle error | $I_\Phi$ |
| | Integral of the yaw angle error | $I_\Psi$ |

**Table 3.** Controls of the aircraft model.

| Model | Control Name | Symbol |
|---|---|---|
| Longitudinal | Commanded load factor | $n_{z,c}$ |
| Lateral | Commanded lateral acceleration | $n_{y,c}$ |
| | Commanded roll angle | $\Phi_c$ |

# 4 Results

## 4.1 Simulation Scenario

The maneuver used to evaluate the proposal in the present paper consists of minimizing the heading $\Psi$ of the aircraft at a fixed final instant $t_f = 10$ s. Such a maneuver corresponds to maximizing the turn of the aircraft nose in the horizontal plane towards the clockwise sense. Constraints are imposed on the variables related to the excursions and rates of the actuators as indicated in Table 4. The commanded roll angle is also limited to avoid unrealistic reference values, thus $\Phi_c \in [-45, 45]$ deg. Moreover, the final roll angle was set to $\Phi(t_f) = 0$ deg and the roll $\omega_x$ and yaw $\omega_z$ rates were subject to terminal constraints $\omega_x(t_f) = \omega_z(t_f) = 0$ deg/s, aiming at returning the aircraft to a leveled flight condition at the end of the maneuver.

For the discretization employed in the optimization problems the time interval $[0, t_f]$ was sampled with $N = 500$ points at a regular interval. However, for the case of the proposed MILP approach, such a quantity of samples entails a large number of binary variables, which are linked to the computational demands for solving the optimization problem. On the other hand, sampling with lower frequency might compromise the capability of predicting accurately the system dynamics, especially of the fastest modes. Therefore, as a compromise solution, the binary variables were kept constant for 10 samples, enabling the real-valued variables to be sampled at a suitable frequency and at the same time reducing the number of binary decision variables to one tenth.

**Table 4.** Constraints on the actuators for the evaluation maneuver.

| Variable Name | Symbol | Minimal value | Maximal value |
|---|---|---|---|
| Left aileron deflection | $\xi_l$ | $-2$ deg | 2 deg |
| Left aileron rate | $\dot{\xi}_l$ | $-26$ deg/s | 26 deg/s |
| Right aileron deflection | $\xi_r$ | $-20$ deg | 20 deg |
| Right aileron rate | $\dot{\xi}_r$ | $-26$ deg/s | 26 deg/s |
| Rudder deflection | $\zeta$ | $-29$ deg | 27 deg |
| Rudder rate | $\dot{\zeta}$ | $-20$ deg/s | 20 deg/s |

A time limit of 120 s was imposed for the MILP solution, i.e., if after this period the optimal solution was not yet determined, the solver returned the feasible solution with the lowest cost so far, if any was available.

## 4.2 Simulation Results with the Linearized Model

The results using the standard optimal control and MILP modeling can be seen in Fig. 1 for the heading $\Psi$, roll $\Phi$ and sideslip $\beta$ angles, as well as the commanded roll $\Phi_c$ angle. The achieved final values of the heading are $\Psi(t_f) = -9.2$ deg imposing the fault as constraints and $\Psi(t_f) = -28.4$ deg with the MILP approach. This difference can be attributed to a less conservative usage of the roll angle with the usual modeling approach, since it does not achieve values lower than $-20$ deg, whereas with the MILP approach the minimum value is lower than $-40$ deg. The sideslip angle is kept low throughout the maneuver with both approaches.

Figure 2 depicts the actuator deflections and rates. Both approaches respect the constraints. However, the MILP scheme enables an asymmetric usage between the left (faulty) and right (healthy) ailerons. Indeed, the right aileron is driven to its lower limit of $-20$ deg between 0 and 2 s. In contrast, without the MILP formulation, the right aileron is steered only between $-2$ and 2 deg. It is important to remark that the MILP approach preserved the constraints imposed on the left aileron, remaining between $-2$ and 2 deg. Moreover, one can see that the availability of more actuator authority in the right aileron leads the MILP solution to use the rudder more intensively, as larger sideslip angle variations are seen with the more aggressive curve flown.

## 4.3 Nonlinear Simulation

For validation purposes, the inputs obtained from the MILP solution were applied to the nonlinear model around the trimmed condition. It is important to remark that this model, besides being nonlinear, involves also the complete dynamics of the aircraft, including the longitudinal movement. The results are presented and discussed in the present subsection.

The heading achieved in the nonlinear simulation can be seen in Fig. 3 to be lower in absolute value in the nonlinear simulation, reaching $\Psi(t_f) = -26.1$ deg, a reduction of 2.3 deg in the span as compared to the linear simulation. However, this remains substantially higher in absolute value when compared to the one obtained when the MILP formulation was not used. Regarding the roll angle, no considerable difference can be noticed in Fig. 3. On the other hand, the sideslip angle can be seen to reach slightly higher absolute values in the nonlinear simulation, albeit still acceptable.

In Figure 4, it can be seen that the left aileron deflection remains at the lower bound for a longer period in the nonlinear simulation as compared to the results with the linear model. Moreover, the right aileron deflection follows the same profile obtained in the linear simulation, with small differences due to different amplitudes and durations of the oscillations in the rate associated to this aileron.

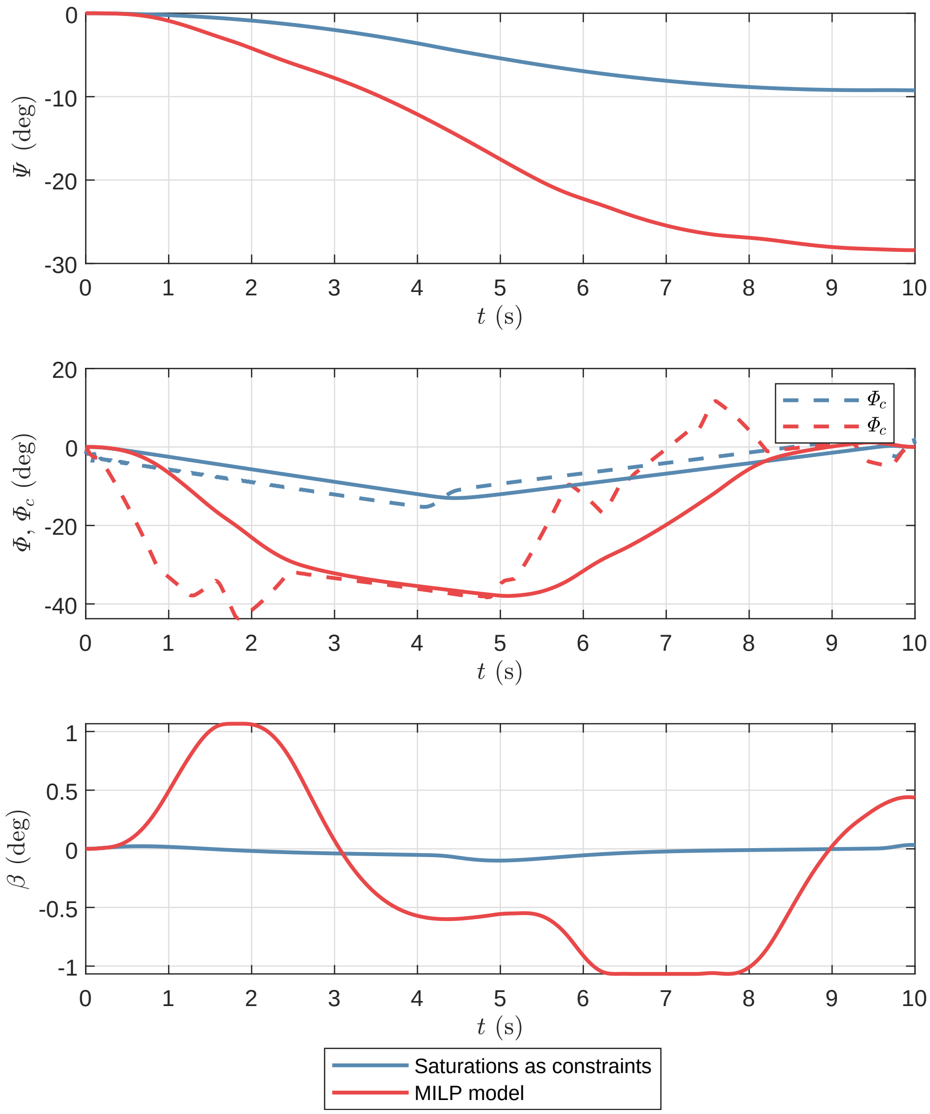


**Fig. 1.** Commands and outputs treating saturation as constraints and with the proposed approach.

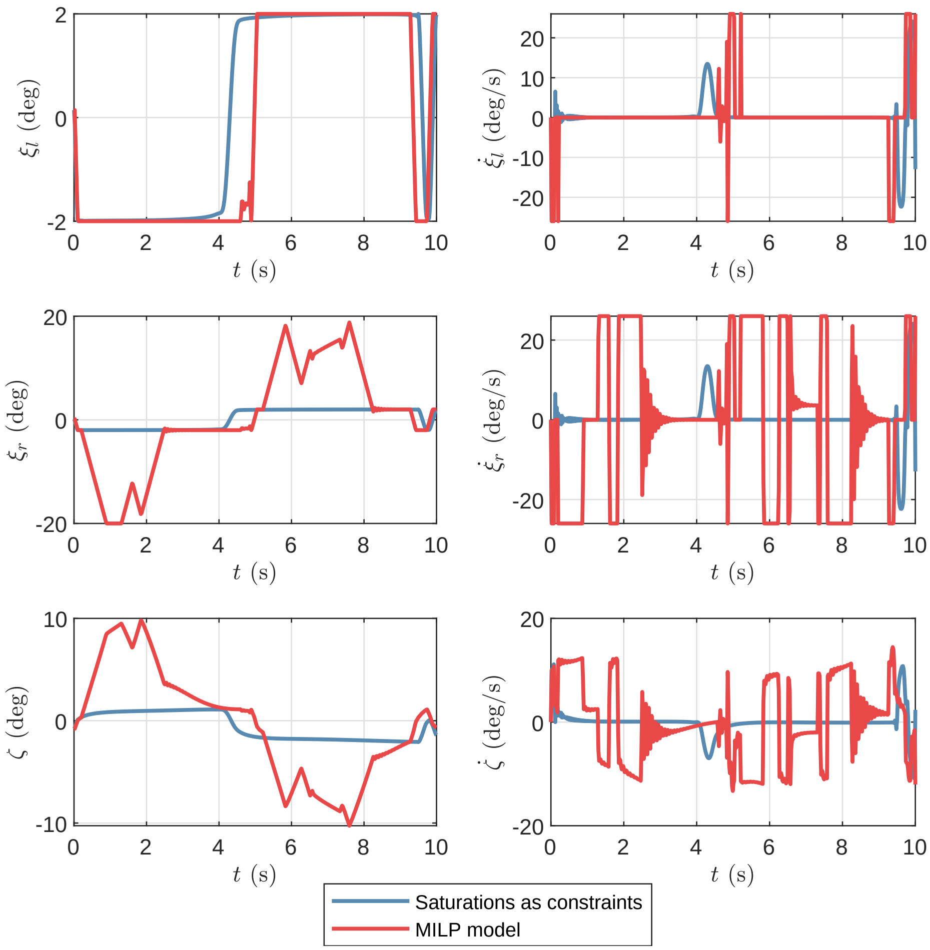


**Fig. 2.** Actuator deflections and rates treating saturation as constraints and with the proposed approach.

The same applies for the rudder. Overall, one can ascertain that the nonlinear simulation confirms the applicability of the controls determined by the proposal and their superior performance in terms of the minimization of the heading.

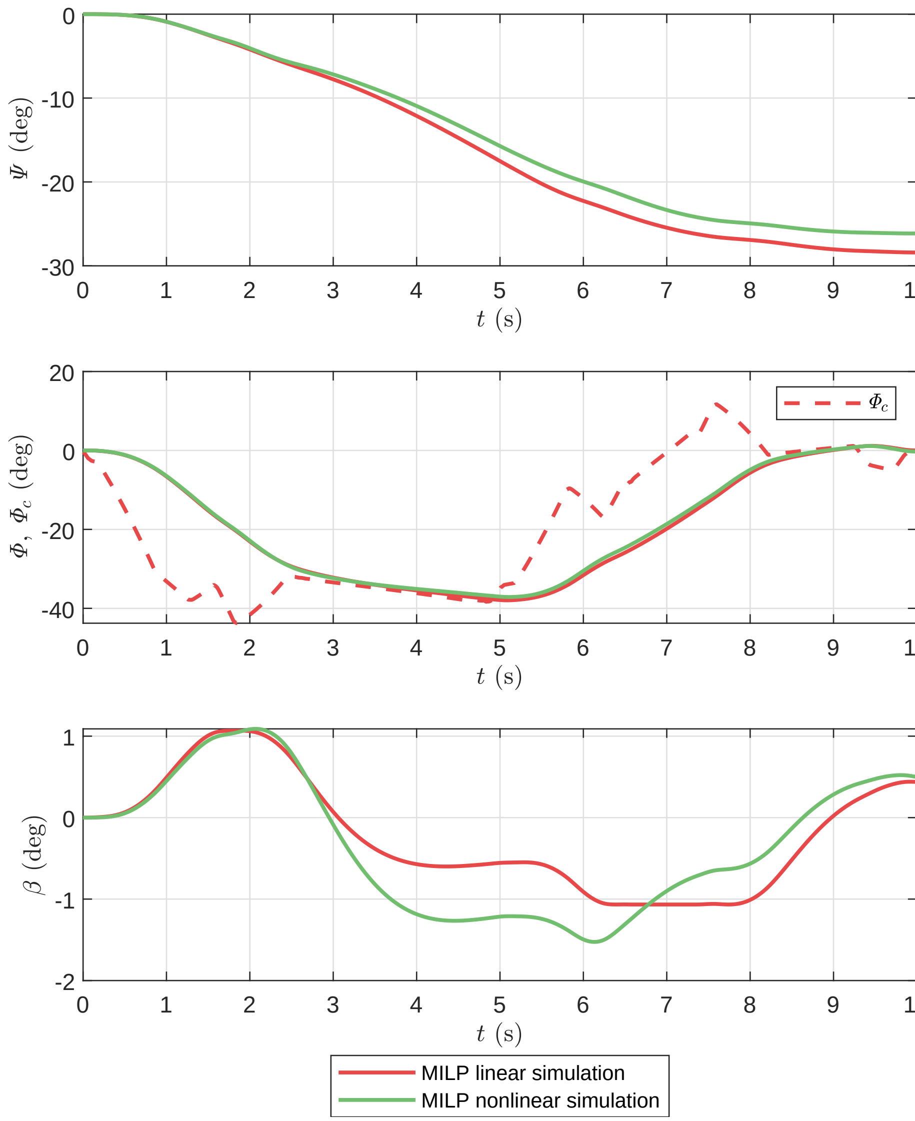


**Fig. 3.** Commands and outputs with the proposed approach simulated with the linear and nonlinear models.

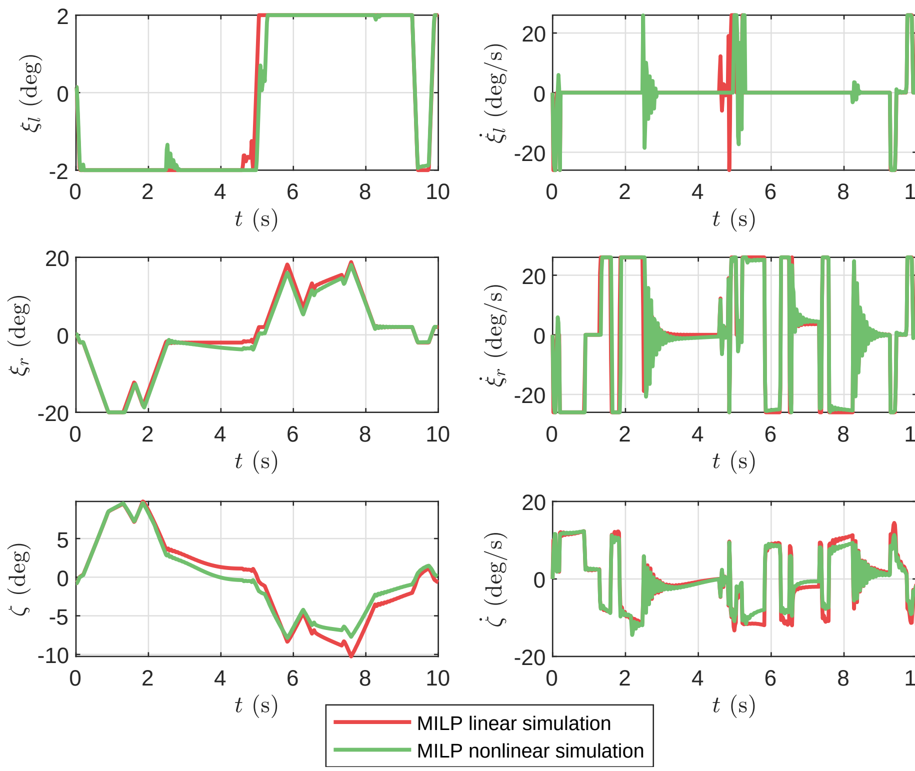


**Fig. 4.** Actuator angles and rates with the proposed approach simulated with the linear and nonlinear models.

# 5 Conclusion and Future Work

In the present work a MLD formulation for modeling internal limits (rate and position) for actuation systems was developed. Under this approach the logical conditions were implemented through a MILP formulation with binary variables. The additional degree of freedom enabled by this formulation results in an improved solution compared to the standard optimal control formulation in the simulation example of the lateral movement of a general transport aircraft. On the other hand, the proposed MILP encoding yields a higher computational burden.

Future work could involve increasing the computational efficiency for solving the resulting MILP problem e.g. through the techniques proposed in [9, 11] for reducing the number of binary variables in the MILP encoding.

# References

1. Agarwal, A., Bhat, S., Gray, A., Grossmann, I.E.: Automating mathematical program transformations. In: Carro, M., Peña, R. (eds.) Practical Aspects of Declarative Languages. PADL 2010. Lecture Notes in Computer Science, vol. 5937, pp. 134–148. Springer, Berlin, Germany (2010). https://doi.org/10.1007/978-3-642-11503-5_12
2. Ahmad, H., Young, T., Toal, D., Omerdic, E.: Control allocation with actuator dynamics for aircraft flight controls. In: 7th AIAA ATIO Conf, 2nd CEIAT Intl Conf on Innov and Integr in Aero Sciences, 17th LTA Systems Tech Conf followed by 2nd TEOS Forum, p. 7828. American Institute of Aeronautics and Astronautics (2007). https://doi.org/10.2514/6.2007-7828
3. Bemporad, A., Morari, M.: Control of systems integrating logic, dynamics, and constraints. Automatica **35**(3), 407–427 (1999). https://doi.org/10.1016/S0005-1098(98)00178-2
4. Cotorruelo, A., Limon, D., Garone, E.: Output admissible sets and reference governors: Saturations are not constraints! IEEE Transactions on Automatic Control **65**(3), 1192–1196 (2020). https://doi.org/10.1109/tac.2019.2921672
5. Garey, M.: Computers and intractability: a guide to the theory of NP-completeness. W.H. Freeman, San Francisco (1979)
6. Garrett, N.J., Best, M.C.: Model predictive driving simulator motion cueing algorithm with actuator-based constraints. Vehicle System Dynamics **51**(8), 1151–1172 (2013). https://doi.org/10.1080/00423114.2013.783219
7. Gerdts, M.: Optimal control of ODEs and DAEs. De Gruyter textbook, Walter de Gruyter GmbH Co. KG (2012). https://doi.org/10.1515/9783110249996
8. Pachter, M., Chandler, P., Mears, M.: Control reconfiguration with actuator rate saturation. In: Proceedings of 1995 American Control Conference (ACC95), vol. 5, pp. 3495–3499. American Autom Control Council (1995). https://doi.org/10.1109/acc.1995.533786
9. Prodan, I., Stoican, F., Olaru, S., Niculescu, S.I.: Enhancements on the hyperplanes arrangements in mixed-integer programming techniques. Journal of Optimization Theory and Applications **154**(2), 549–572 (2012). https://doi.org/10.1007/s10957-012-0022-9
10. Rundqwist, L., Ståhl-Gunnarsson, K., Enhagen, J.: Rate limiters with phase compensation in jas 39 gripen. In: 1997 European Control Conference (ECC), pp. 3944–3949 (1997). https://doi.org/10.23919/ECC.1997.7082737
11. Vielma, J.P., Nemhauser, G.L.: Modeling disjunctive constraints with a logarithmic number of binary variables and constraints. Mathematical Programming **128**(1-2), 49–72 (2009). https://doi.org/10.1007/s10107-009-0295-4